Dynamic Mechanical Analysis of Ethylene–Propylene–Diene Monomer Rubber and Styrene–Butadiene Rubber Blends

T. Muraleedharan Nair,[1] M. G. Kumaran,[2] G. Unnikrishnan,[3] V. B. Pillai[4]

[1]*Rubber Testing Laboratory, Common Facility Service Centre (Department of Industries, Government of Kerala), Industrial Nagar P.O., Changanacherry 686 106, Kerala, India*
[2]*Rubber Research Institute of India, Kottayam 686 009, Kerala, India*
[3]*National Institute of Technology, Calicut 673 601, Kerala, India*
[4]*Naval Physical and Oceanographic Laboratory, Kochi 682021, India*

Received 7 May 2008; accepted 24 August 2008
DOI 10.1002/app.29367
Published online 19 December 2008 in Wiley InterScience (www.interscience.wiley.com).

ABSTRACT: The effects of blend ratio, crosslinking systems, and fillers on the viscoelastic response of ethylene–propylene–diene monomer (EPDM)/styrene–butadiene rubber (SBR) blends were studied as functions of frequency, temperature, and cure systems. The storage modulus decreased with increasing SBR content. The loss modulus and loss tangent results showed that the EPDM/SBR blend vulcanizate containing 80 wt % EPDM had the highest compatibility. Among the different cure systems studied, the dicumyl peroxide cured blends exhibited the highest storage modulus. The reinforcing fillers were found to reduce the loss tangent peak height. The blend containing 40 wt % EPDM showed partial miscibility. The dispersed EPDM phase suppressed the glass-transition temperature of the matrix phase. The dynamic mechanical response of rubbery region was dominated by SBR in the EPDM–SBR blend. The morphology of the blend was studied by means of scanning electron microscopy. The blend containing 80 wt % EPDM had small domains of SBR particles dispersed uniformly throughout the EPDM matrix, which helped to toughen the matrix and prevent crack propagation; this led to enhanced blend compatibility. © 2008 Wiley Periodicals, Inc. J Appl Polym Sci 112: 72–81, 2009

Key words: elastomers; glass transition; miscibility; rubber; vulcanization

INTRODUCTION

One of the remarkable features of polymers is their sharply expressed viscoelastic properties that give rise to a unique complex of fundamental physical and mechanical properties.[1] Polymers display properties of both elastic solids and liquids. This leads to a specific relationship between the stress (σ), which changes according to a periodic law for viscoelastic bodies, and the strain (ε):

$$\sigma = E^*\varepsilon \tag{1}$$

where E^* is the complex modulus of elasticity:

$$E^* = E' + iE'' \tag{2}$$

The real part of the modulus of elasticity (E') is called the *dynamic modulus of elasticity* or the *storage modulus*, and the imaginary part (E'') is called the *loss modulus*. The phase shift between the sinusoidally varying stress and strain is expressed as

$$\tan\delta = E''/E' \tag{3}$$

where $\tan\delta$ is the mechanical loss factor or the loss tangent. One of the simplest and most reliable ways of determining these components is through dynamic mechanical analysis (DMA).

Dynamic mechanical testing is a versatile and sensitive technique that enables the complete exploration of the relaxation mechanisms in viscoelastic materials.[1,2] The most common use of DMA is the determination of the glass-transition temperature (T_g), where the molecular chains of a polymer obtain sufficient energy, usually from thermal sources, to overcome the energy barriers for segmental motion. This is also the region where the maximum loss of applied energy is observed, usually as a peak in the traces of the loss factor versus frequency or temperature. Several interesting studies on the dynamic mechanical properties of various systems are available in literature.[3–9]

The objective of this article is to discuss the effects of blend composition, crosslinking systems, and fillers on the dynamic mechanical behavior of

Correspondence to: T. M. Nair (mdnair05@yahoo.com).

ethylene–propylene–diene monomer (EPDM)/styrene–butadiene rubber (SBR) blends as studied by DMA. The dynamic mechanical properties, including storage modulus, loss modulus, and damping characteristics, were examined. The morphology of the blends was also studied with scanning electron microscopy (SEM).

EXPERIMENTAL

Materials

In this study, EPDM-502 was supplied by Herdillia Unimers, Ltd. (Mumbai, India), and SBR-1502 was supplied by India Rubber Chemicals (Kottayam, India). The rubber chemicals we used, including sulfur, zinc oxide, stearic acid, mercaptobenzothiazyl disulfide (MBTS), and tetramethyl thiuram disulfide (TMTD), were commercial grade.

Blend preparation

Blends of EPDM and SBR, with different crosslinking systems and fillers, were prepared on a two-roll mixing mill (Indian Expeller, Noida, India) (diameter = 150 mm, speed of the slow roll = 24 rpm, gear ratio = 1 : 16). The mastication of each polymer and the subsequent blending and compounding were done between the hot rolls of the mill at 80°C. The basic recipes used for compounding are given in Table I. The compounds were designated as E_0S, $E_{20}S$, $E_{40}S$, $E_{60}S$, $E_{80}S$, and $E_{100}S$, where E stands for EPDM rubber, the subscripts indicate the weight percentage of EPDM in the blends, and S designates the vulcanizing system sulfur.

The rheometric parameters of the blends, such as the optimum cure time (time to achieve 90% of the cure), maximum and minimum torques, and scorch time (time for a 2-dNm increase in torque), were obtained with a Scarabaeus GmbH rheometer (Germany). The vulcanization of the blends was carried out on a hydraulic press (platen size = 8 × 8 in^2) under a pressure of 1500 psi at a temperature of 160°C.

DMA

The viscoelastic properties of the blends were measured with a dynamic mechanical thermal analyzer (Q800, TA Instruments, New Castle, DE) in the frequency range 0.1–100 Hz. The temperature of the testing was in the range −70 to 120°C, and the amplitude was 15 μm. A single cantilever clamp was used to mount the samples. Compression-molded samples with dimensions of 25 × 8 × 3 mm^3 were used for testing.

Morphology

The morphology of the blends was analyzed with SEM. A Jeol JSM-5600 LV scanning electron microscope (Jeol, Ltd., Tokyo, Japan) and a Jeol JFC-1200 fine coater were also used for the morphological study of the blends.

RESULTS AND DISCUSSION

Storage modulus

The magnitude and nature of changes in the dynamic storage moduli were determined by both the intermolecular and intramolecular interactions, which have a significant influence on the different physical states of a polymer system.[1,2,10]

TABLE I
Compounding Recipe

Ingredient	Sulfur system	DCP system	Mixed system (sulfur and DCP)	HAF	GPF	Silica	Clay
Polymer (blends)[a]	100.0	100.0	100.0	100.0	100.0	100.0	100.0
Zinc oxide	4.0	4.0	4.0	4.0	4.0	4.0	4.0
Stearic acid	1.5	1.5	1.5	1.5	1.5	1.5	1.5
MBTS	1.25	1.25	1.25	1.25	1.25	1.25	1.25
TMTD	1.00	1.00	1.00	1.00	1.00	1.00	1.00
Sulfur	2.50	—	—	2.5	2.5	2.5	2.5
DCP	—	4	—	—	—	—	—
Sulfur and DCP	—	—	2.0+2.0	—	—	—	—
HAF	—	—	—	10.0	—	—	—
GPF	—	—	—	—	10.0	—	—
Silica	—	—	—	—	—	10.0	—
Clay	—	—	—	—	—	—	10.0

The values are parts per hundred parts of rubber by weight. In the sample codes, HB is used for HAF, GB is used for GPF, S is used for sulfur, SI is used for silica, and CL is used for clay.

[a] EPDM/SBR blends of various compositions.

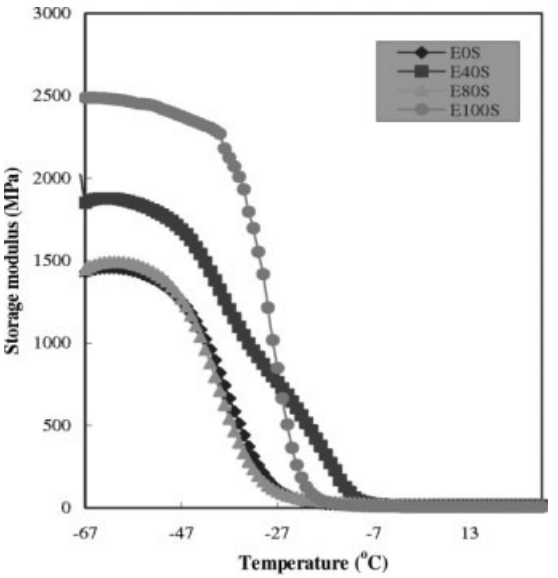

Figure 1 Effect of temperature (−67 to 30°C) on the storage modulus of sulfur-cured EPDM, SBR, and EPDM/SBR blends as a function of the blend ratio at a frequency of 10 Hz.

Effect of the blend ratio

Figure 1 shows the effect of the blend ratio on the storage modulus of the sulfur-cured EPDM, SBR, and their blends at different temperatures. At lower temperatures, below T_g, pure EPDM (E_{100}) showed the highest modulus, whereas pure SBR (E_0) showed the lowest. This was correlated with the different structural characteristics of EPDM and SBR. The modulus in the glassy region was the effect of intermolecular interactions.[2,10] EPDM, being crystalline and having better intermolecular interactions in the absence of any bulky groups, such as the phenyl group in SBR, showed the highest modulus. The blends $E_{80}S$ and $E_{40}S$ showed intermediate values.

Both the rubbers and their blends showed single transitions, which indicated the absence of immiscible phases. However, the blend $E_{40}S$ showed a broad transition with a shoulder in the middle, which indicated the presence of heterogeneous zones in the blend. This indicated the partial miscibility of the blend with this ratio.[11] This is also indicated the lower mechanical properties of the blend, which were due to the poor interfacial adhesion, as reported in our earlier article.[12]

In the rubbery region (above T_g), E_0S showed the highest modulus, followed by $E_{40}S$ and $E_{80}S$, and the lowest was shown by $E_{100}S$. The modulus in the rubbery region is contributed by the ability of the macromolecules to resist the intermolecular slippage. As a result, SBR, having stronger molecular interactions than the nonpolar EPDM, showed the highest modulus. The blends with the SBR matrix ($E_{40}S$) again showed a higher modulus than those with the EPDM matrix ($E_{80}S$) for the same reason.

Effect of the curing agents

The effect of the curing agents on the storage modulus of the $E_{80}S$ composition cured by different agents, namely, sulfur, dicumyl peroxide (DCP), and mixed agents, are shown in Figure 2. The peroxide-cured blend ($E_{80}P$) exhibited a higher storage modulus in the glassy region than the sulfur-cured blend ($E_{80}S$). This was attributed to the stiff C—C cross-links in $E_{80}P$ vis-à-vis the more flexible C—S_x—C bonds in $E_{80}S$. Figure 3 shows the influence of the temperature on the storage modulus of E_{80} cured with three curing agents, namely, sulfur, DCP, and mixed agents, above ambient conditions (30–120°C). The storage modulus was highest for sulfur-cured systems compared to DCP and mixed-agent cured systems.

Effect of the fillers

Figures 4 and 5 represent the effect of fillers on the storage moduli of the EPDM/SBR blend $E_{80}S$. The incorporation of reinforcing fillers increased the modulus, and the effect was visible in the various plots of $E_{80}S$. Among carbon black fillers, high-abrasion furnace black (HAF) blends were found to exhibit a higher modulus than general-purpose furnace black (GPF) blends. This was attributed to the reinforcing effect of HAF, which provided the highest modulus in the blend, followed by GPF,

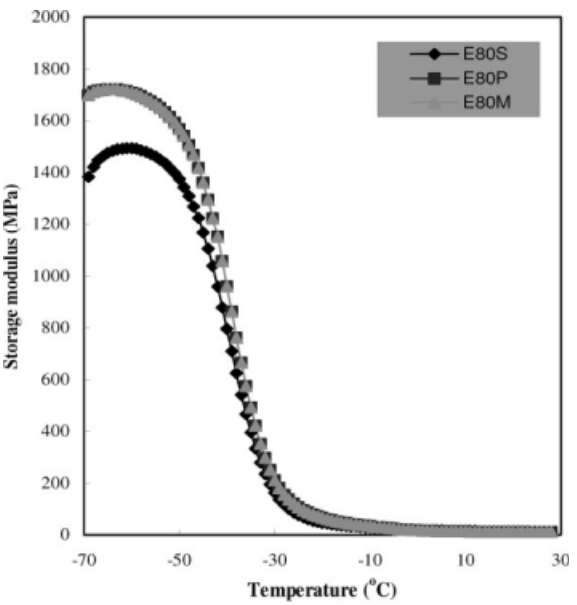

Figure 2 Effect of temperature (−70 to 30°C) on the storage modulus of $E_{80}S$, $E_{80}M$, and $E_{80}P$ at a frequency of 10 Hz.

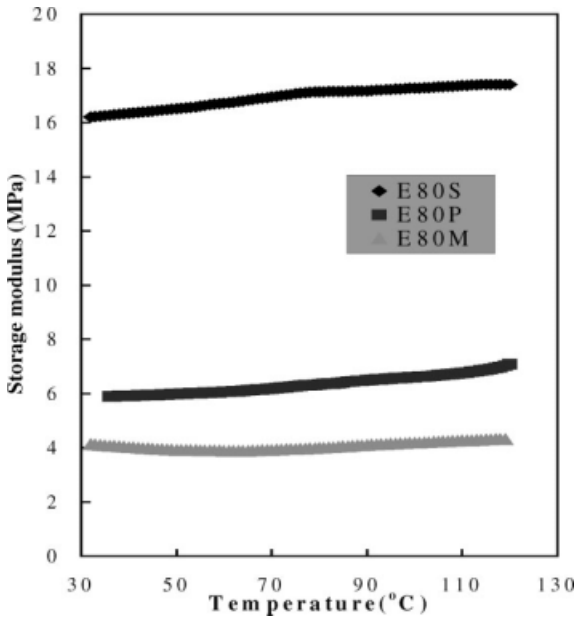

Figure 3 Effect of temperature (30–120°C) on the storage modulus of E_{80} cured by sulfur, DCP, and mixed systems at a frequency of 10 Hz.

silica, and clay.[13] HAF, a better reinforcing agent, interacted well with the blends and showed a high modulus. Among the nonblack fillers examined, clay blends exhibited lower moduli compared to silica blends. This was due to the nonreinforcing nature of clay, as it had no interaction with the rubber matrix. Although silica was also a reinforcing filler, in this case, its effect was less because of the fact that the interaction between the polar silica filler and the

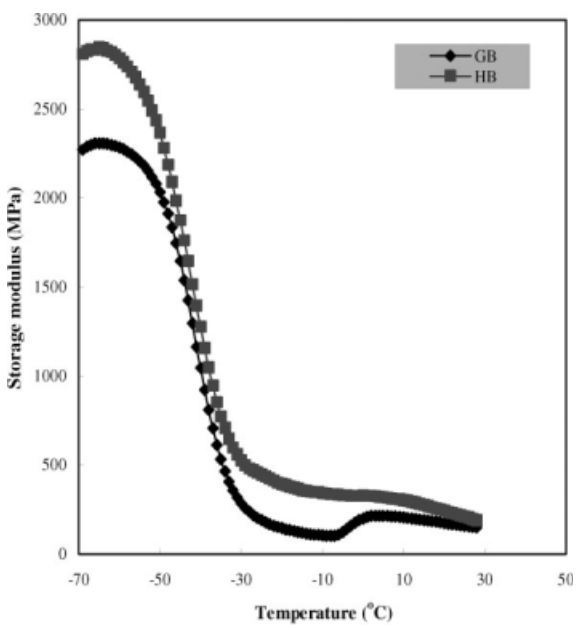

Figure 4 Effect of temperature (−70 to 30°C) on the storage modulus of E_{80}S10HB and E_{80}S10GB at a frequency of 10 Hz.

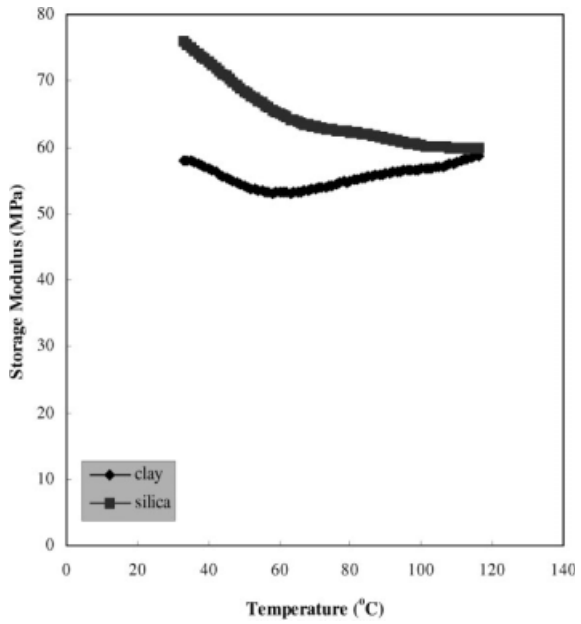

Figure 5 Effect of temperature (30–120°C) on the storage modulus of a clay- and silica-filled EPDM/SBR blend (E_{80}S) at a frequency of 10 Hz.

mostly nonpolar EPDM or SBR matrix was very poor. GPF was a semireinforcing filler and, hence, showed a modulus between those of HAF and silica.

Loss modulus

Effect of the blend ratio

The effect of the blend ratio on the loss modulus of sulfur-cured EPDM, SBR, and their blends in different ratios are shown in Figure 6. The pure rubbers and the blend E_{80}S, except E_{40}S, showed single glass-transition peaks in the loss modulus versus temperature peaks, which again indicated the presence of a homogeneous phase in the blends. E_{40}S exhibited two peaks at −36 and −15°C, which again indicated the presence of two phases. The peak at −36°C corresponded to SBR (pure SBR also had the transition at −36°C), and the one at −15°C related to EPDM. Pure EPDM had a glass transition at −28°C. The difference may have been due to the compacting of the EPDM macromolecules dispersed as particles in the SBR matrix, which restricted the molecular movement. Any type of molecular interactions that affect the molecular motion leads to a shift in the transition to higher temperature, as more energy is needed to overcome the interactions.[10,11] The influence of temperature (30–120°C) on the loss modulus of the unvulcanized blend components EPDM, SBR, and the blend E_{80} were determined and are shown in Figure 7. The figure shows that pure EPDM showed an increase in the loss modulus, whereas the values of SBR and the blend remained almost constant with increasing temperature.

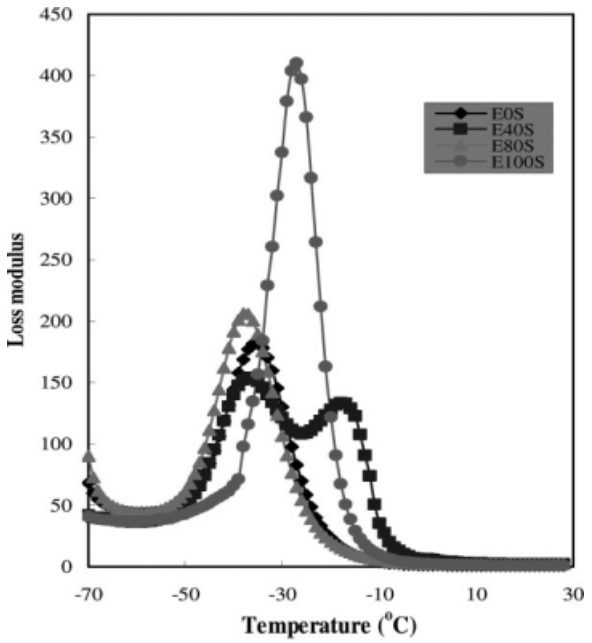

Figure 6 Effect of temperature (−70 to 30°C) on the loss modulus of sulfur-cured EPDM, SBR, and EPDM/SBR blends at a frequency of 10 Hz.

Effect of the curing agents

Figure 8 shows the influence of the different curing agents (sulfur, DCP, and mixed agents) on the loss modulus of the blend E_{80}. The E_{80} blend did not show any significant effect on the loss modulus behavior with different curing agents, as compared to the storage modulus value.

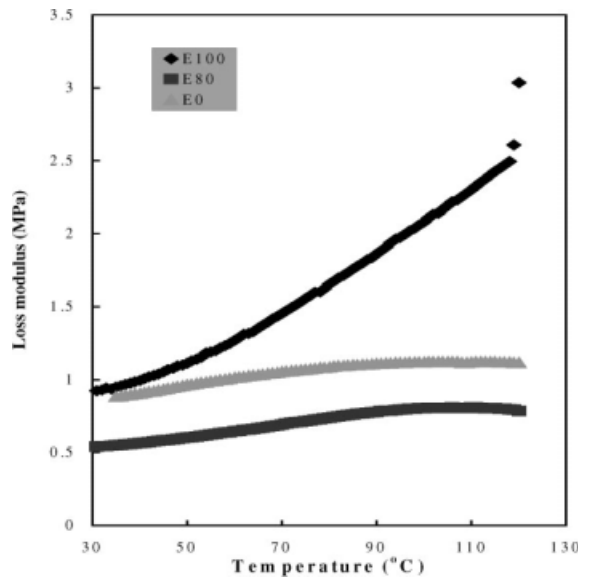

Figure 7 Effect of temperature (30–120°C) on the loss modulus of an unvulcanized blend (E_{80}), EPDM, and SBR at a frequency of 10 Hz.

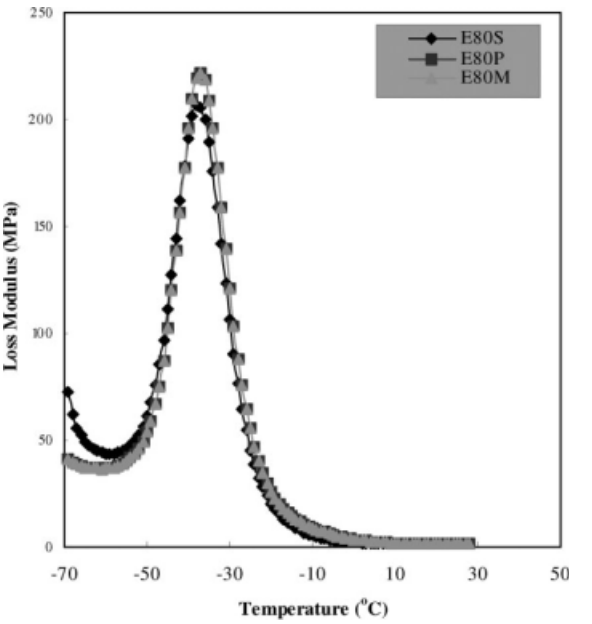

Figure 8 Effect of temperature (−70 to 30°C) on the loss modulus of sulfur, DCP, and mixed systems at a frequency of 10 Hz.

Effect of the fillers

The effect of temperature on the loss modulus of the filler-loaded EPDM/SBR blend $E_{80}S$ is presented in Figures 9 and 10. As observed for the storage modulus, the blend containing the reinforcing filler HAF showed the highest loss modulus compared to GPF. This was attributed to the energy loss occurring at the rubber–filler interface consequent to the good

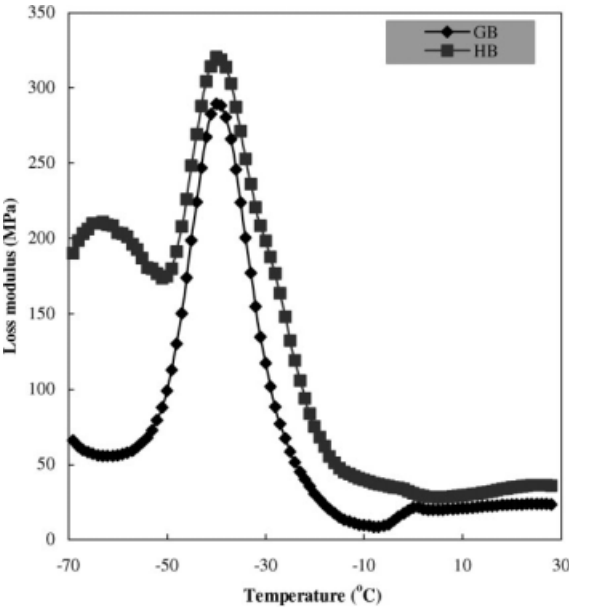

Figure 9 Effect of temperature (−70 to 30°C) on the loss modulus of carbon black filled $E_{80}S10HB$ and $E_{80}S10GB$ at a frequency of 10 Hz.

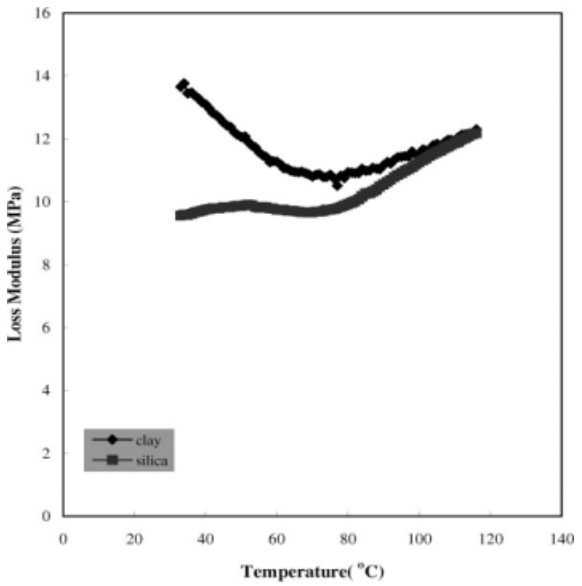

Figure 10 Effect of temperature (30–120°C) on the loss modulus of E_{80}S10CL and E_{80}S10SI at a frequency of 10 Hz.

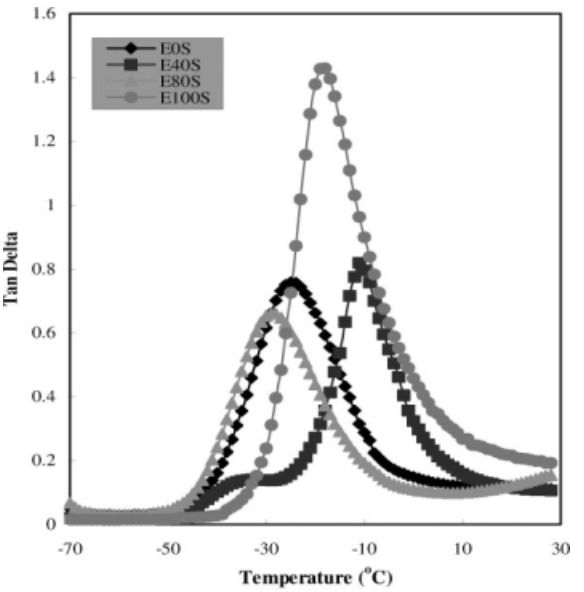

Figure 11 Effect of temperature on the loss tangent (tan δ) of EPDM/SBR blends as a function of the blend ratio at a frequency of 10 Hz.

rubber–filler interaction.[13] At room temperature, the loss modulus remained low and more or less constant for all of the filled systems. The loss modulus values and the corresponding T_g's of the filled and unfilled blend E_{80} cured in different curing systems are presented in Table II. The T_g values were not affected by different curing systems, whereas carbon blacks changed the T_g from −37 to −40 in HAF.

Loss tangent

The loss tangent is a ratio and corresponds to the energy lost as heat per energy absorbed and returned by the system per unit cycle. As the temperature increases, the damping goes through a maximum in the transition region and then decreases in the rubbery region. The damping is low below T_g because the chain segments are frozen in that region. Below T_g, the deformations are primarily elastic, and the molecular motions resulting in viscous flow are less. Above T_g, the damping is low because the molecular segments are free to move and there is no resistance to flow. The damping is high in the transition region because of the initiation of micro-Brownian motion of the macromolecules and their stress relaxation, although not all of the segments will be able to take part in such relaxation together.

TABLE II
Values of the Loss Modulus and T_g of the Filled and Unfilled E_{80} Blends Cured with Sulfur, DCP, and Mixed Systems at 10 Hz

Sample code	Loss modulus (MPa)	T_g (°C)
E_{80}S	205.7	−37
E_{80}P	221.8	−37
E_{80}M	221.8	−37
E_{80}S10HB	320.5	−40
E_{80}S10GB	288.5	−39

Effect of the blend ratio

The effect of the blend ratio on the loss tangent is shown in Figure 11. Pure EPDM and SBR showed glass-transition peaks at −18 and −24°C, respectively (Table III). The blend E_{80} also showed a single transition at −28°C, which indicated miscibility between the components. When the EPDM/SBR blend ratio was 40/60, there was a large peak at −11°C, followed by a small shoulder at −35°C, which were attributed to SBR and EPDM, as described earlier in the case of the loss modulus plots. The presence of a shoulder rather than a clear peak indicated partial miscibility rather than true immiscibility.[11] Although SBR was the matrix in this case, its transition was rather suppressed by EPDM, as observed in many blends, because of the compact

TABLE III
Comparison of the T_g Values of the Sulfur-Cured EPDM/SBR Blends Based on the Peak Values of the Loss Tangent and Loss Modulus at 10 Hz

	T_g (°C)	
Blend	Loss tangent peak	Loss modulus peak
E_{100}S	−18	−27
E_{80}S	−28	−37
E_{40}S	−11	−36 and −17
E_0S	−24	−35

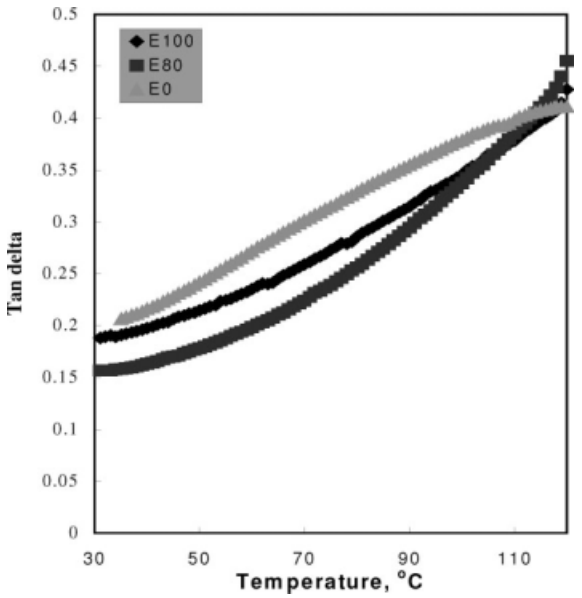

Figure 12 Effect of temperature (30–120°C) on the loss tangent (tan δ) of unvulcanized blend components EPDM and SBR and blend E_{80} at a frequency of 10 Hz.

EPDM particles dispersed in the matrix. A comparison of the T_g value of the sulfur-cured EPDM/SBR blends based on the peak values of the loss tangent and loss modulus at 10 Hz is given in Table III.

Figure 12 shows that with the increase in temperature above ambient conditions, the loss tangent values increased in all three uncured systems: EPDM, SBR, and the E_{80} blend. The loss tangent values in all of these systems seemed to be closer with increasing temperature; SBR had higher values in the early stages of heating, but the values continuously increased in the blend E_{80} with increasing temperature.

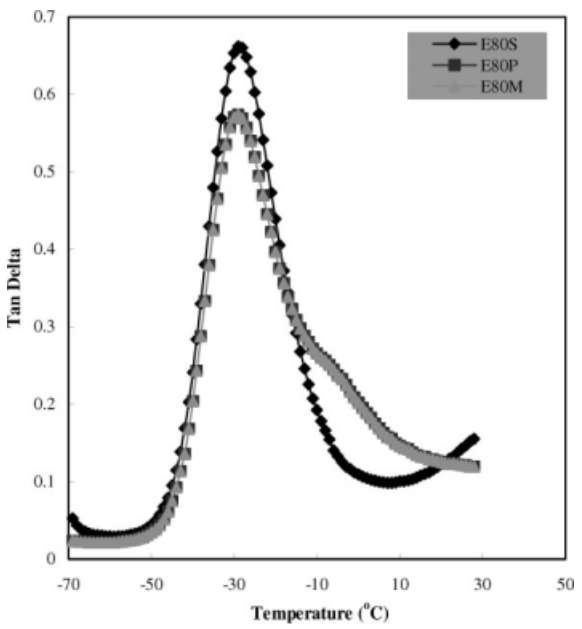

Figure 13 Effect of temperature on the loss tangent (tan δ) of E_{80}S, E_{80}P, and E_{80}M.

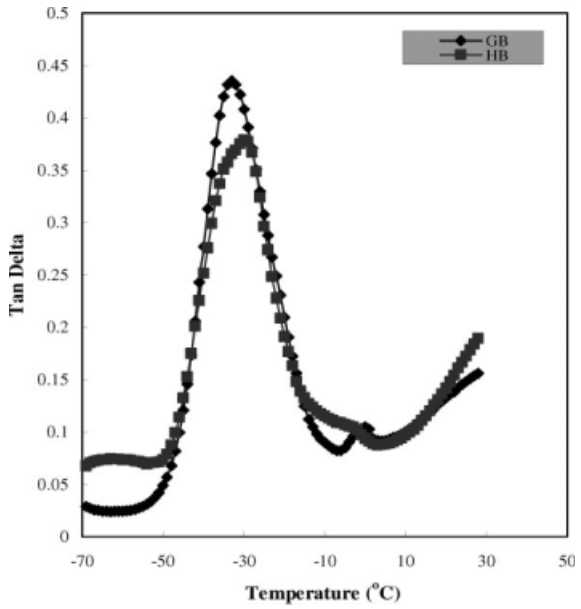

Figure 14 Effect of temperature (−70 to 30°C) on the loss tangent (tan δ) of E_{80}S10HB and E_{80}S10GBat a frequency of 10 Hz.

Effect of the curing agents

The effect of the temperature on the loss tangent of the E_{80} blend cured by different curing agents is presented in Figure 13. The E_{80} blend when cured with sulfur showed a single transition, which indicated a homogeneous composition. However, E_{80}P and E_{80}M

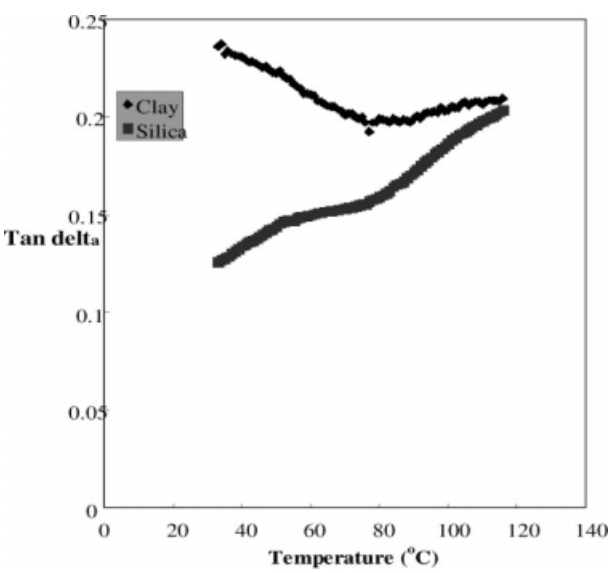

Figure 15 Effect of temperature (30–120°C) on the loss tangent (tan δ) of E_{80}S10CLand E_{80}S10SI at a frequency of 10 Hz.

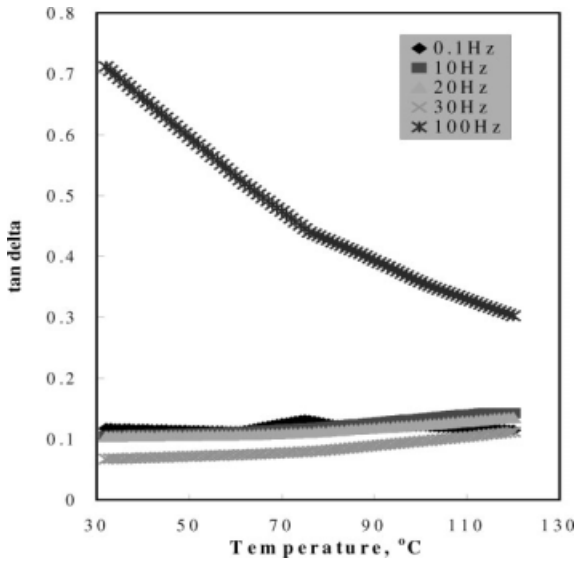

Figure 16 Effects of various frequencies on the loss tangent (tan δ) of $E_{80}S$ above the ambient temperature (30–120°C).

exhibited a shoulder at −7°C after the primary transition at −28°C, the latter corresponding to SBR. The shoulder may have been due to some heterogeneous phases of the crosslinked EPDM where crystallization was effected consequent to peroxide curing in $E_{80}P$ and $E_{80}M$. Peroxide curing is known to improve the chances of crystallization in EPDM as compared to sulfur curing, as the macromolecules are aligned and brought closer because of intermolecular C—C bond formation.

Effect of the fillers

The effect of the temperature on the loss tangent of the filled (black and nonblack) EPDM/SBR blend $E_{80}S$ is shown in Figures 14 and 15. The addition of reinforcing fillers reduced the loss tangent peak height, whereas nonreinforcing fillers increased the value. The loss tangent at T_g was 0.66 for the pure $E_{80}S$ blend, whereas the values were 0.38 and 0.43, respectively, for the highly reinforcing HAF and semireinforcing GPF filled blends.

Effect of the frequency

The effect of different frequencies on the dynamic mechanical properties of $E_{80}S$ above room temperature was also examined. Figure 16 shows the influence of different frequencies, 0.1, 10, 20, 30, and 100 Hz, on the loss tangent of $E_{80}S$.The loss tangent values, except those at a frequency of 100 Hz, were parallel to the temperature axis. This was attributed to the fact that, at higher frequencies, the polymer chain did not have sufficient time for molecular relaxation.

Morphology

SEM has been successfully used by researchers to study the morphology of polymer blends.[14–17] The SEM photographs of unfractured specimens of the E_{80} blends cured with DCP, sulfur, and mixed systems are presented in Figure 17(a–c), respectively. Figure 17(a) shows the SEM micrographs of the DCP-cured blend $E_{80}P$, which had a flakelike structure filled with pores, which ultimately led to lower mechanical properties. As shown in Figure 17(b), the phase domains were globular shaped and were of relatively uniform size. The domains of the SBR particles were dispersed in the EPDM matrix, which prevented crack growth in the blend during tensile stress. In the mixed system, $E_{80}M$ [Fig. 17(c)], the particles were more uniform in size, and they were interwoven with the globular structure.

The SEM micrographs shown in Figure 18(a–f) explain the morphology of the tensile fractured surfaces of the sulfur-cured EPDM/SBR blends at different blend ratios. Figure 18(a) shows the SEM

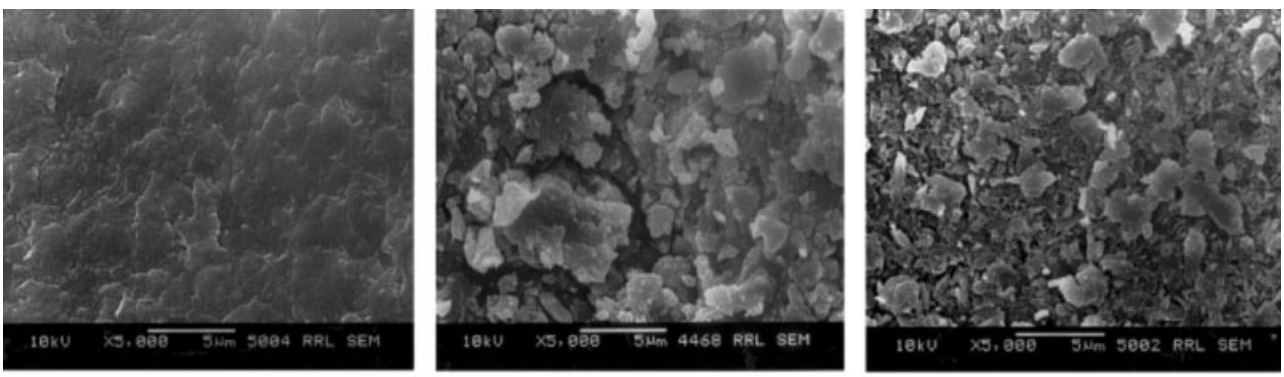

Figure 17 SEM photographs of cryogenically fractured specimens of EPDM/SBR blends.

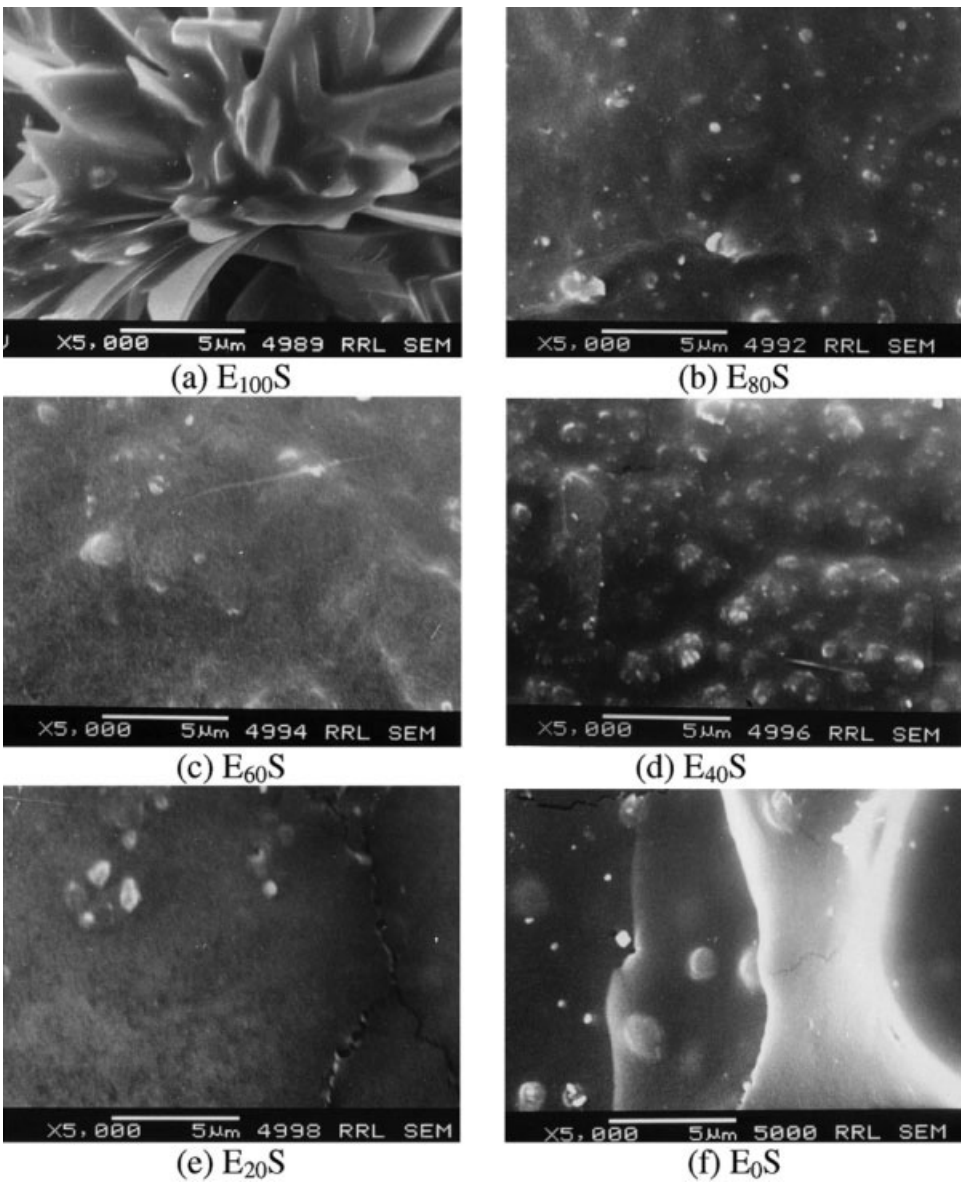

Figure 18 SEM images of tensile-fractured specimens of EPDM/SBR blends: (a) $E_{100}S$, (b) $E_{80}S$, (c) $E_{60}S$, (d) $E_{40}S$, (e) $E_{20}S$, and (f) E_0S.

micrographs of pure EPDM vulcanized by sulfur with a characteristic ductile failure and rough surface. The absence of a dispersed phase caused easy crack propagation and poor tensile properties. Figure 18(b) shows the changes in morphology with the introduction of SBR into EPDM. SEM of the blend $E_{80}S$ showed that small domains of the dispersed phase SBR were distributed relatively uniformly throughout the matrix. Earlier studies[18–20] showed that crack bifurcation in blends can be prevented by a small and uniformly distributed minor phase in the matrix. The particle size of the minor phase in the blend $E_{80}S$ was small and uniform, which helped to toughen the matrix and prevent crack propagation. The miscibility of the blend was found to increase.

The results of DMA were complementary to this observation. As SBR particles increased, the agglomeration of the dispersed phase particles occurred. Consequently, the miscibility of the blends decreased, and the crack propagation increased in the $E_{60}S$, $E_{40}S$, and $E_{20}S$ blends, as shown in Figure 18(c–e). Figure 18(f) shows the SEM results of pure SBR. The morphology studies showed that the best distribution of the dispersed phase existed in the E_{80} composition.

Theoretical modeling

To assess the behavior of the EPDM/SBR blends from the DMA data, different theoretical models

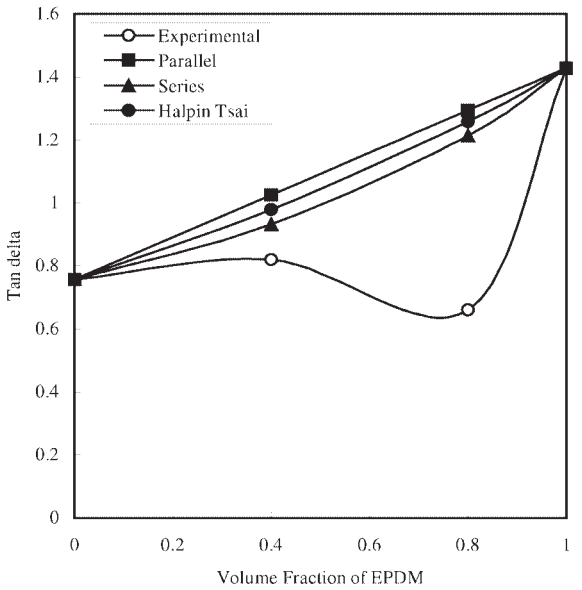

Figure 19 Experimental and theoretical curves of loss tangent (tan δ) peaks of sulfur-cured EPDM/SBR blends.

were used. The various models applied included parallel, series, and Halpin Tsai.[21]

The curves resulting from the theoretical models and that of the experimental data for the variation of the loss tangent at 30°C with the volume fraction of EPDM are given in Figure 19. The experimental value of the loss tangent was found to be lower than that of the theoretical predictions. This was due to the presence of extranet work materials present in the blends. The experimental model was found to fit well with the series model. The parallel model and Halpin Tsai model showed the upper bound over the entire compositions.

CONCLUSIONS

DMA is an effective tool for evaluating the miscibility of polymer blends. DMA of EPDM/SBR blends was carried out as a function of blend composition, crosslinking systems, and fillers over a wide range of temperatures and frequencies. The single T_g obtained from the loss tangent peak for the blend $E_{80}S$ showed that the system was miscible. The two separate loss tangent peaks, obtained during DMA, in the blend $E_{40}S$ indicated that the miscibility of the system decreased with increasing SBR content.

Reinforcing black fillers increased the modulus and decreased the loss tangent peak. The morphology studies of the EPDM/SBR blends were complementary to the DMA results.

References

1. Perepechko, I. Acoustic Methods of Investigating Polymers; Mir: Moscow, 1975.
2. Murayama, T. Dynamic Mechanical Analysis of Polymeric Materials; Materials Science Monograph 1; Elsevier Science: New York, 1978.
3. Murayama, T. Dynamic Mechanical Analysis of Polymeric Materials; Elsevier: New York, 1977.
4. Kevin, P. Dynamic Mechanical Analysis—A Practical Introduction; CRC: New York, 1999.
5. Read, B. E.; Brown, G. D. The Determination of Dynamic Mechanical Properties of Polymers and Composites; Wiley: New York, 1978.
6. Ferry, J. Viscoelastic Properties of Polymers; Wiley: New York, 1980.
7. Karger-Kocsis, A.; Kiss, L. Polym Eng Sci 1987, 27, 254.
8. Khonakdar, H. A.; Wagenknecht, U.; Jafari, S. H.; Hassler, R.; Eslami, H. Adv Polym Technol 2004, 23, 307.
9. Mas, J.; Vidaurre, A.; Mesegner, J. M.; Romero, F.; Pradas, M. M.; Ribelles, J. L. G.; Maspoch, M. L. L.; Santana, O. O.; Pages, P.; Perez-Folch, J. J Appl Polym Sci 2002, 83, 1507.
10. Ferry, J. D. Viscoelastic Properties of Polymers; Wiley: New York, 1980.
11. MacKnight, W. J.; Karasz, F. E.; Fried, J. R. In Polymer Blends; Paul, D. R.; Newman, S., Eds.; Academic: New York, 1978; Vol. 1, Chapter 5, p 185.
12. Muraleedharan Nair, T.; Kumaran, M. G.; Unnikrishnan, G. J Appl Polym Sci 2004, 93, 2606.
13. Payne, A. R. In Reinforcement of Elastomers; Kraus, G., Ed.; Interscience: New York, 1965.
14. Gent, A. N.; Pulford, C. T. R. J Mater Sci 1984, 19, 3612.
15. Kuriakose, B.; De, S. K. J Mater Sci 1985, 20, 1864.
16. Bhagavan, S. S.; Tripathy, D. K.; De, S. K. J Mater Sci 1987, 6, 157.
17. Thomas, S.; Kuriakose, B.; Gupta, B. R.; De, S. K. J Mater Sci 1986, 21, 711.
18. Hu, R.; Dimonic, V. L.; El-Aasser, M. S.; Pearson, R. A.; Hiltner, A.; Mylonakis, S. G.; Sperling, L. H. J Polym Sci Part B: Polym Phys 1997, 35, 1501.
19. Thomas, S.; Gupta, B. R.; De, S. K. J Vinyl Technol 1987, 9, 71.
20. Fukahori, Y. Int Polym Sci Technol 1982, 76, 9.
21. Nielson, L. E. Rheol Acta 1974, 13, 86.